Tropical Journal of Pharmaceutical Research April 2023; 22 (4): 795-804
ISSN: 1596-5996 (print); 1596-9827 (electronic)

Available online at http://www.tjpr.org
http://dx.doi.org/10.4314/tjpr.v22i4.12

Original Research Article

Cytotoxic and alpha amylase-inhibitory metabolites from *Tagetes minuta*: *In vitro* evaluation and docking studies

Gamal A Mohamed[1]*, Ali A Alqarni[1], Hossam M Abdallah[1], Abdelsattar M Omar[2,3], Sabrin RM Ibrahim[4,5]

[1]Department of Natural Products and Alternative Medicine, [2]Department of Pharmaceutical Chemistry, Faculty of Pharmacy, [3]Center for Artificial Intelligence in Precision Medicines, King Abdulaziz University, Jeddah 21589, Saudi Arabia, [4]Department of Chemistry, Preparatory Year Program, Batterjee Medical College, Jeddah 21442, Saudi Arabia, [5]Department of Pharmacognosy, Faculty of Pharmacy, Assiut University, Assiut 71526, Egypt

For correspondence: **Email: gahussein@kau.edu.sa; **Tel:** +966-597636182*

Sent for review: 13 January 2023 *Revised accepted: 28 March 2023*

Abstract

Purpose: *To investigate the cytotoxic and alpha-amylase inhibitory (AAI) potential of methanol (MeOH) extract of T. minuta and its isolated metabolites.*

Methods: *Phytochemical investigation of MeOH extract of the aerial parts of T. minuta was accomplished using SiO_2 and Rp-18 column chromatography (CC). The structures of the isolated metabolites were determined and verified based on various data, in addition to comparison with literature data. The metabolites were assessed for cytotoxic potential against HepG2, MCF-7, and HCT116 cell lines utilizing sulphur rhodamine B (SRB) assay. The in vitro AAI potential of the metabolites were also assayed, and the findings were confirmed using results from molecular docking studies.*

Results: *One thiophene (compound 1), one coumarin (compound 2), and three phenolic compounds (compounds 3-5) were isolated and characterized. Compound 1 exhibited a marked cytotoxic effect (IC_{50} values: 2.7 – 7.3 µM) on HepG2, MCF-7, and HCT116 cell lines, relative to doxorubicin (IC_{50} values: 0.18 - 0.60 µM), whereas compound 2 had a moderate cytotoxic effect on MCF-7 (IC_{50} 17.7 µM). Besides, compounds 4 and 5 produced potent AAI effects, with IC_{50} values of 12.3 and 9.2 µM, respectively, and 91.8 and 94.7 % inhibition, respectively), when compared to acarbose (94.7 % inhibition and IC_{50} of 7.1 µM). Interestingly, the in vitro AAI and in silico results were in agreement with each other. Compounds 5 and 4 had more negative docking scores (-13.655 and -12.135 kcal/mol, respectively) than the native inhibitors, myricetin (-12.155 kcal/mol) and acarbose (-15.105 kcal/mol).*

Conclusion: *These results suggest that T. minuta is a valuable source of anti-diabetic and cytotoxic metabolites. However, there is a need to validate these results through additional in vivo and in vitro investigations.*

Keywords: *Tagetes minuta, Asteraceae, Flavonoids, Alpha-amylase inhibition, Cytotoxic potential*

Tropical Journal of Pharmaceutical Research is indexed by Science Citation Index (SciSearch), Scopus, Web of Science, Chemical Abstracts, Embase, Index Copernicus, EBSCO, African Index Medicus, JournalSeek, Journal Citation Reports/Science Edition, Directory of Open Access Journals (DOAJ), African Journal Online, Bioline International, Open-J-Gate and Pharmacy Abstracts

INTRODUCTION

Chronic diseases such as cancer, diabetes, and cardiovascular and chronic lung diseases represent huge health burdens worldwide [1]. Diabetes and cancer are crucial health concerns and major causes of death globally [1]. Diabetes is a metabolic disorder characterized by

prolonged hyperglycemia. It has been estimated that 422 million suffered from diabetes worldwide in 2014, while 1.6 million deaths in 2016 were directly related to diabetes [2].

Diabetes elevates the risk of developing various severe health-threatening conditions due to the impairment of the function of several organs such as the heart, kidneys, nerves, blood vessels, and skin. This results in vascular complications such as neuropathy, retinopathy, and nephropathy, in addition to hypertension, stroke, and atherosclerosis, all of which are responsible for most diabetes-related deaths [1,2]. In addition, high blood glucose levels boost carcinogenesis and cancer cell proliferation. Diabetes is a common illness in cancer patients. It is a risk factor for certain cancers such as liver, pancreatic, colon, endometrial, and breast cancers [3]. Diabetic cancer patients face rare challenges because the simultaneous usage of certain chemotherapies or steroids may exacerbate pre-existing diabetes, or induce new diabetes [3]. These patients are at high risk of cancer-linked mortality and an elevated risk of different infections and infection-associated mortality and morbidity [1]. Diverse medications are prescribed for treating these disorders. However, these drugs are expensive, noxious, and associated with serious and undesirable side effects [1]. Therefore, it is necessary to identify natural metabolites that may be used to protect against or prevent the pathogenesis of these diseases.

Natural metabolites have remarkably contributed to drug discovery, either directly or through laboratory modification of their basic skeletons [4]. Interestingly, phytochemicals from fruits and vegetables have been found to lessen the prevalence of various types of cancers and age-related pathological disorders and attenuate chronic human illnesses [5]. Furthermore, many studies have demonstrated the potent antioxidant capacities of these phytochemicals and their potential to counteract oxidative stress-linked disorders through multiple pathways [4,5].

The *Tagetes* genus (Asteraceae) comprises about 56 species which include 29 perennials and 27 annuals [6]. *Tagetes minuta* L. (marigold) is one of the most common species of this genus in Chile, Argentina, Bolivia, Paraguay, Peru, and Saudi Arabia [7]. Indeed, it grows as a noxious weed in more than 35 countries [6,7]. Traditionally, this plant is applied for treating diverse ailments, including coughs, calluses, chest infections, congestion, catarrh, bunions, cuts, wounds, and colds [8,9]. The leaf infusion is utilized for treating intestinal and stomach diseases. The plant has gained great industrial interest because of its unique-aroma essential oil (*Tagetes* oil) which is globally in high demand in the perfumery and flavour industries [8,9].

Indeed, *Tagetes* oil is used as flavour in various food products such as cola and alcoholic beverages, mayonnaise, candy, margarine, puddings, frozen-dairy desserts, vegetable oil, condiments, gelatines, and baked foods [8, 9]. The plant is associated with a variety of bio-activities such as antimicrobial, antioxidant, insecticide, alpha-amylase inhibitory, antispasmodic, antiseptic, sedative, anti-parasitic, acaricidal, and anti-inflammatory properties [6-9]. Previous investigations on *T. minuta* resulted in the identification of different classes of metabolites such as monoterpenes (e.g., acyclic and mono- and bicyclic), sesquiterpenes, flavonoids, sterols, phenolics, and thiophenes [8-10].

In this study, the aerial parts *T. minuta* were investigated as part of the continued search for ideal candidates for treatment of chronic illnesses. The aim was to provide more information about the binding affinities of the compounds to the enzyme active site.

EXPERIMENTAL

General

Spectrometer Hitachi-300 was utilized for UV measurements. Electrospray Ionisation-Mass Spectrometry (ESI-MS) measurements were done on an LCQ-DECA mass spectrometer. Nuclear Magnetic Resonance (NMR) analysis was performed using the 600 AVANCE-BRUKER instrument. Sephadex LH-20, RP-18, and SiO_2 60 were utilized for chromatographic analysis.

Plant materials, extraction, and isolation

The aerial parts of Tagetes *minuta* L. were collected from Fifa mountain (Jizan governorate, KSA) in July 2020. The authentication of the plant was confirmed as stated formerly [11]. A voucher specimen (Reg no. TM-4-2020) was preserved at the herbarium of Natural Products and Alternative Medicine Department. The dried-powdered aerial part (750.0 g) was extracted with MeOH (7.5 L $\times$ 4). Then, the resultant extract was vacuum-concentrated to yield 54.0 g of a dark-greenish residue. The latter was chromatographed on VLC using a solvent system of $CHCl_3$/*n*-hexane/EtOAc/MeOH. This resulted in four fractions: TMH (*n*-hexane fraction, 12.6 g); TMC ($CHCl_3$ fraction, 8.6 g); TME (EtOAc fraction, 5.9 g), and

TMM (MeOH fraction, 19.5 g). Chromatographic separation on SiO_2 and Rp-18 CC led to the isolation of compounds **1**–**5** (Figure 1).

Docking analysis

All molecular docking analyses were performed using Maestro software (Schrodinger, LLC, New York, version 13.2.128, MMshare Version 5.8.128, Release 2022-2, Platform Windows-x64).

Preparation of ligands

To prepare the investigated compounds for docking, the 2D structures were converted into 3D structures using Schrodinger Maestro suite's LigPrep program. The OPLS4 force field was used to generate tautomeric forms and ionization states (pH 7.0 ± 2.0 [12].

Preparation of protein structure of α-amylase (AA)

The protein structure of human α-amylase (PDB ID: 4GQR) was prepared using the Wizard program for protein preparation. Hydrogens were added, disulphide bonds were created, and seleno-methionine residues were converted to methionine. Side chains and missing loops were completed using Prime [13]. Moreover, the bond orders were assigned. Using Epik, the hit state was generated at pH 7.0 ± 2.0. At pH 7.0, H-bonds were optimized utilizing PROPKA. Restrained minimization was done utilizing an OPLS4 forcefield.

Generation of receptor grid

A grid box was formed around the binding place of the minimized-human α-amylase protein structure that had the co-crystallized inhibitor (PDB-ID: 4GQR). The binding region was assigned by selecting myricetin (a native inhibitor) as the centroid with a 10 Å radius. Non-polar atoms were set for Van der Waals radii scaling factor to 1 and 0.25 partial charge cut-off.

Ligand docking

The ligands were docked using Glide program of the Schrodinger suite, using the extra precision (XP) protocol. Docking quality was assessed using a re-docking study of the native inhibitor myricetin [13].

Induced-fit docking (IFD)

This is a protocol used to dock ligands using the Glide docking algorithm which includes complex Glide redocking, Prime refinement, and binding score calculation [13]. To obtain the best pose, the centroid of the ligand with the least GlideEModel value which was obtained through ligand docking was used.

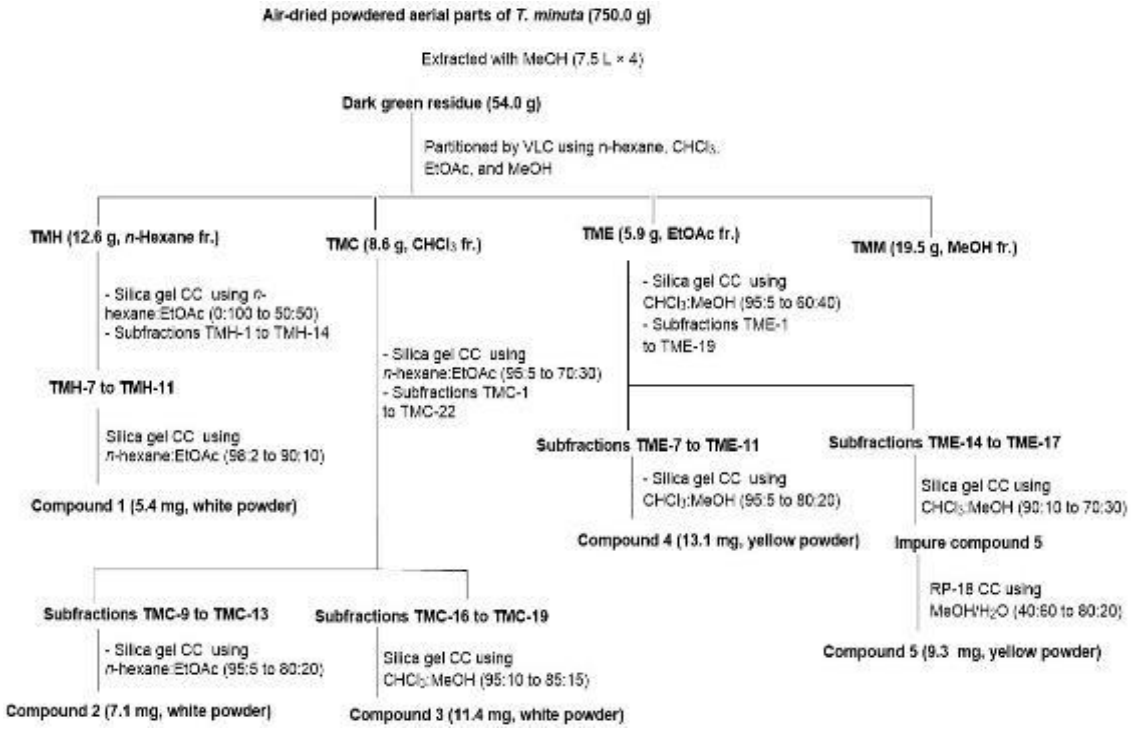

Figure 1: Extraction and separation procedures used for compounds **1**–**5**

Residues that were within 5Å of the ligand pose underwent Prime Refinement. Glide redocking was carried out using the Extra Precision (XP) method, and the OPLS4 all-atom force field was utilized. After each run, the ligand was saved in ten different poses, and the best pose was assessed using the Ligand Efficiency (LE) parameter. The LE parameter normalized the binding energy to molecular size, which enhanced the Van der Waals and hydrophobic interactions by rescaling the high-energy binding of the ligands with high molecular weights [13].

RESULTS

In this work, the MeOH extract was partitioned between *n*-hexane, $CHCl_3$, and EtOAc. Each fraction was separated utilizing SiO_2 and RP-18 columns to isolate ecliptal (5-formyl-2,2`,5`,2``-terthiophene) (**1**) [10]: scopoletin (**2**) [8], *p*-hydroxy benzoic acid (**3**) [14], patuletin (**4**) [15], and patuletin-7- glucoside (**5**) [15]. These identities were assigned using spectral analyses and comparisons with literature (Figure 2).

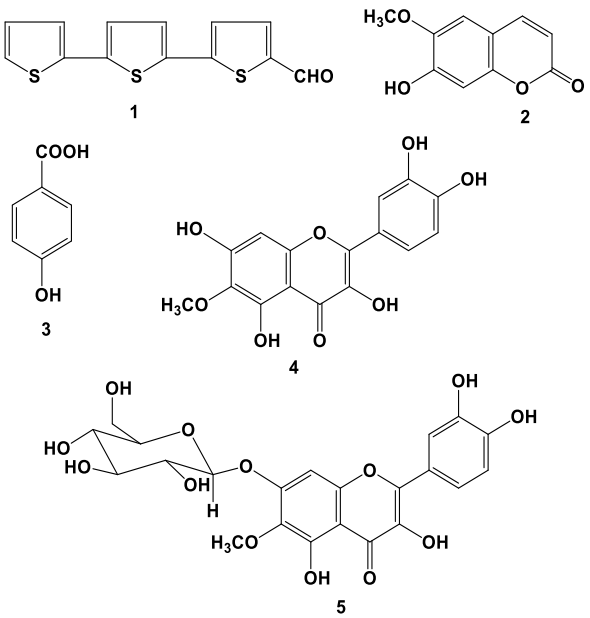

Figure 2: Compounds **1**–**5** isolated from *T. minuta*

The cytotoxic activities of compounds **1**–**5** against HepG2, MCF-7, and HCT116 cell lines were determined. It is worth noting that compound **1** produced a marked cytotoxic effect on all tested cells (IC_{50} values: 2.7 – 7.3 µM) when compared to doxorubicin (IC_{50} values of 0.60, 0.20, and 0.18 µM, respectively); while compound **2** had moderate toxicity against MCF-7 (IC_{50} 17.7 µM). On the other hand, compounds **4** and **5** were moderately cytotoxic (IC_{50} values: 11.7–35.6 µM). However, compound **3** was inactive. Moreover, compounds **1**–**5** were investigated for AAI effectiveness at concentrations of 40, 20, 10, and 5 µM. Compounds **4** and **5** produced potent AAI effects (with IC_{50} value of 12.3 µM and % inhibition of 91.8 for **4,** and IC_{50} of 9.2 µM and % inhibition of 94.7 for **5**), relative to acarbose (IC_{50} of 7.1 µM and % inhibition 97.4). In contrast, compounds **1** and **2** showed moderate effectiveness (IC_{50} of 34.2 µM and % inhibition of 48.1, and IC_{50} 29.8 µM and % inhibition of 50.6, respectively), while compound **3** had weak potential (% inhibition of 38.9 and IC_{50} of 41.2 µM).

Additionally, the AAI activities of the natural compounds were investigated through molecular docking and binding energy analysis.

Glide software was employed to calculate the docking score, Glide calculated Ligand Efficiencies (LE), XP GScore, Glide gscore, Glide emodel, and Prime Energy MMGBSA ΔG values for binding of acarbose and compounds **1**-**5**.

After validating and establishing the docking protocol by reproducing all properties of binding of the experimental structures, the IFD docking protocol was used to test the remaining compounds. The results were evaluated based on the docking score and ligands efficiency (LE), which is a scoring function that considers all the chemical features of atoms involved in the interaction [23]. The calculated binding energy was normalized using LE, relative to the number of heavy atoms that make up the ligand. The docking score based on LE represents affinity. Compound **5** had the strongest binding affinity, with a docking score of -13.655 kcal/mol, relative to acarbose and myricetin which had binding scores of -15.105 kcal/mol and -12.155 kcal/mol, respectively, while compound **4** exhibited a reasonable docking score of -12.135 kcal/mol. The docking score, Glide calculated Ligand Efficiencies (LE), and MM-GBSA values for the tested compounds used in developing the docking model are shown in Table 1. The table includes the title, docking score, Glide LE, XP GScore, Glide gscore, Glide emodel, Prime Energy, and MMGBSA ΔG values for binding of each compound.

Overall, the findings of this study suggest that the natural compound patuletin-7- glucoside, is a promising candidate for the development of a novel α-amylase inhibitor. Further studies are needed for validating these results and exploring the potential of these compounds as antidiabetic agents.

Table 1: Docking score, Glide calculated LE and MM-GBSA ΔG values for the tested compounds

Title	Docking Score (kcal/mol)	Glide LE	XPG Score (kcal/mol)	Glide Gscore (kcal/mol)	Glide Emodel (kcal/mol)	Prime Energy (kcal/mol)	MMGBSA ΔG for binding (kcal/mol)
Acarbose	-15.105	-0.275	-15.105	-15.105	-76.354	-21027	-52.5
Patuletin-7-glucoside (**5**)	-13.655	-0.39	-13.655	-13.655	-92.66	-21237	-53.49
Myricetin	-13.155	-0.572	-13.155	-13.155	-77.908	-21385	-54.89
Patuletin (**4**)	-12.135	-0.506	-12.174	-12.174	-74.357	-21318	-52.75
Scopoletin (**2**)	-5.956	-0.425	-5.969	-5.969	-34.059	-21157	-29.87
Ecliptal (**1**)	-5.73	-0.337	-5.73	-5.73	-42.984	-21161	-42.71
P-Hydroxy benzoic acid (**3**)	-4.097	-0.41	-4.097	-4.097	-24.693	-21156	2.21

DISCUSSION

Tagetes minuta is rich in secondary metabolites [8-11,16]. In this study, 5 compounds were isolated and characterized from various fractions of MeOH leaf extract of the plant. These metabolites comprised one thiophene (compound **1**), one coumarin (compound **2**), one phenolic (compound **3**), and two flavonoids (compounds **4** and **5**). Compound **1** had a potent cytotoxic effect against the tested cell lines, whereas compounds **4** and **5** demonstrated potent AAI capacity. Besides, these metabolites are known to exhibit diverse bioactivities such as anti-microbial, anti-viral, anti-leishmanial, larvicidal, anti-hyperglycaemic, anti-inflammatory, anti-convulsant, insecticidal, antioxidant, cytotoxic, neuroprotective, phototoxic, and nematocidal properties, as well as HIV-1 protease- and cathepsin D-inhibitory potential [8-11,16].

The 2020 global cancer statistics revealed that breast cancer exceeded lung cancer as the most prevalent cancer type, with prevalence values of 11.7 and 11.4 %, respectively, followed by colorectal, prostate, and stomach cancers [17]. The same statistics revealed that colorectal, liver, and breast cancers accounted for 9.4, 8.3, and 6.9 %, respectively, as the prevalent causes of cancer deaths, followed by lung cancer (18 %) [17].

Carbohydrate digestion is initiated by AA which breaks the 1,4-glycosidic-bonds of starch to produce disaccharide and glucose units, leading to post-prandial hyper-glycemia [18]. Therefore, an AA inhibitor such as acarbose delays carbohydrate assimilation and lowers post-prandial glucose levels. Studies have established that traditional medicinal plants are rich reservoirs of phytoconstituents with anti-diabetic potential [19,20].

Computer-aided modelling tools are used to predict interactions between molecules and biotargets. Such modelling has proven to be helpful in gaining insights into the potential bio-activities, mechanisms of action, and modes of binding associated with metabolites [21]. To gain a deeper understanding of the capacities of these compounds to inhibit AA, and to establish correlations among the *in vitro* inhibition results, these compounds were docked against AA, along with myricetin and acarbose.

To build a reliable model that correlated ligand structure with the binding of human AA, the crystal structure of human AA (PDB: 4GQR) published by Williams *et al*. [22] was used to dock the ligands into the AA binding site. The process was started by testing the parameters that could accurately reproduce the X-Ray structure of human pancreatic AA in complex formation with myricetin. To achieve this, myricetin was removed, and then re-docked using the docking procedure as described in the Methods section. Upon completion of this process, the root-mean-square-deviation (RMSD) of the positions of heavy atoms of ligand between favourable poses and crystallographic poses was calculated. Interestingly, the RMSD was as low as 0.1502 Å. This revealed that the docking protocol was efficient and that it produced binding modes with similar poses to the crystallographic poses (Figure 3 A).

Furthermore, the procedure used for the re-docking was re-tested using the IFD protocol. The IFD protocol allows the amino acid residues in the binding pocket to adapt to the presence of the myricetin by mimicking the ligand-protein cross-talk that occurs upon binding. As a result, the RMSD between the crystalized and docked ligand increased to 0.9082 Å due to the slight re-arrangements of functional groups and atoms. However, the overall binding interaction mode remained conserved, as seen in the superimposition of two poses in Figure 3B.

The binding interactions of compounds **1-5** with the active site of the specific protein, i.e., AA, were investigated in the present study. The results revealed that compound **5** formed hydrogen bonds with the amino-acid residues Glu 233, Asp197, and Asp 356 in the active site

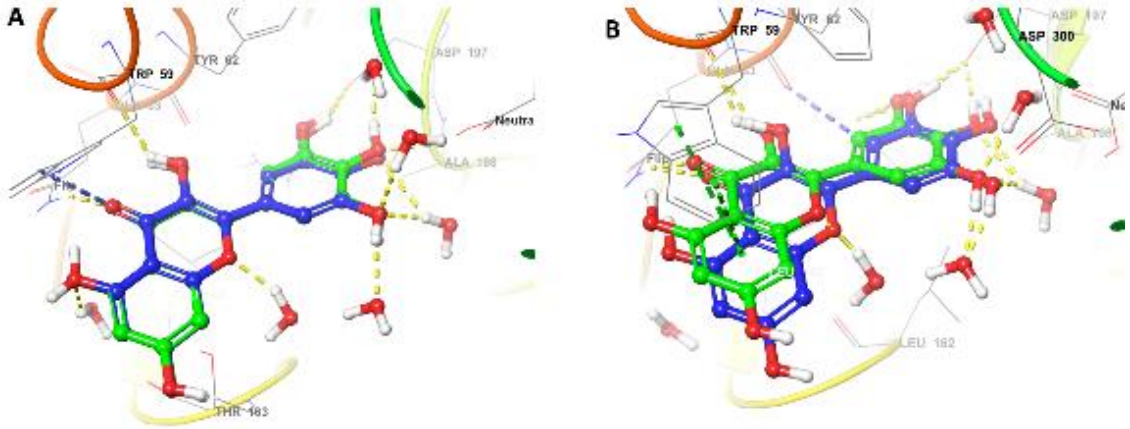

Figure 3: A. Differences in myricetin binding between ligand dockings; **B.** induced-fit docking, relative to the crystal pose (in green)

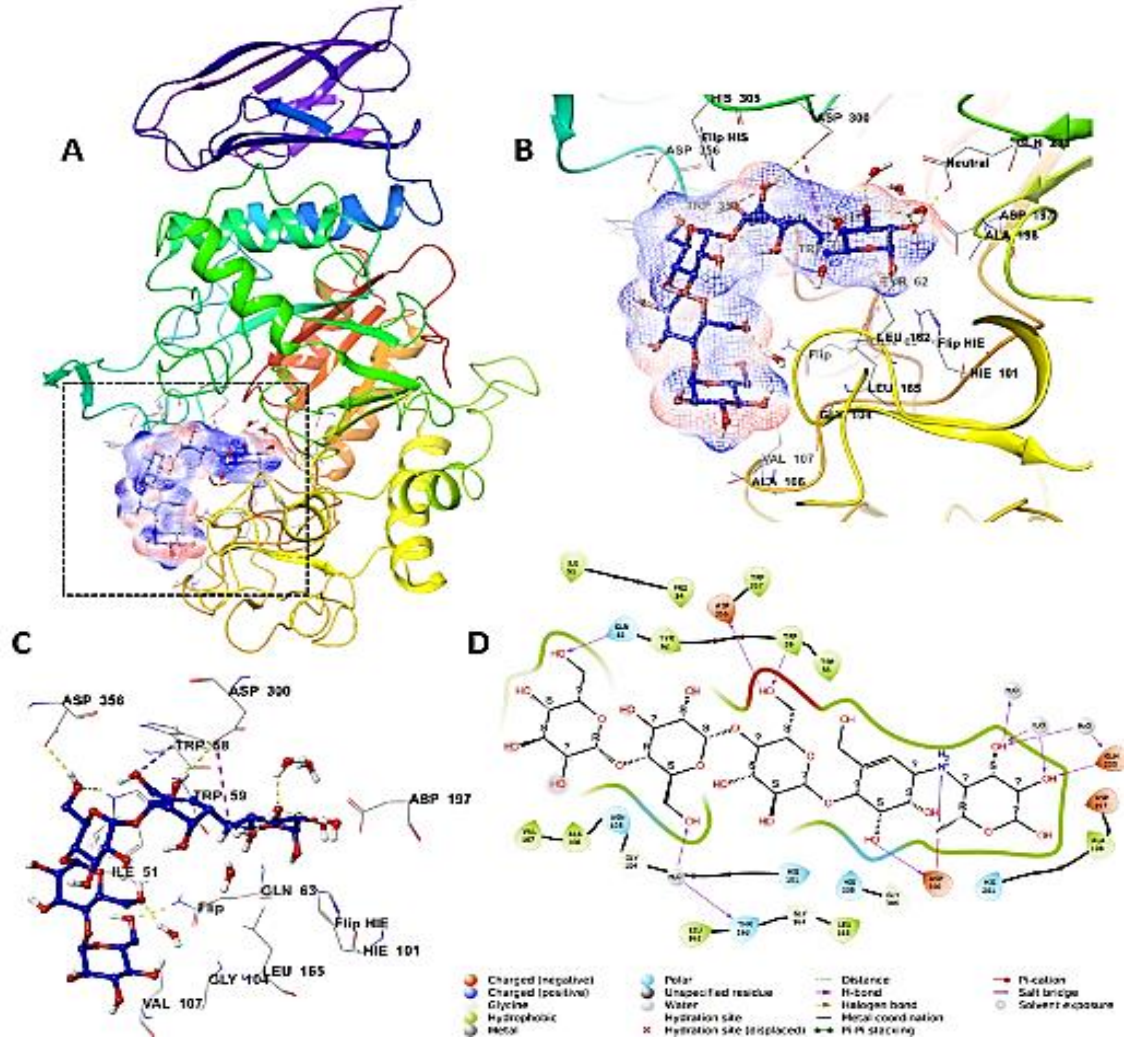

Figure 4: (**A**) Cartoon representation of acarbose in complex with human AA (PDB: 4GQR), with residue position colour scheme and mesh style, and electrostatic potential colour scheme for the ligand (red, white, and blue; minimum electrostatic potential: -0.3, maximum electrostatic potential: +0.3). (**B**) Close-up view of acarbose bound to human AA binding site. (**C**) 3-D representation of the binding interactions: acarbose (green wire representation), amino acid residues (grey wire representation), aromatic hydrogen bonds (violet dots), and hydrogen bonds (yellow dots). (**D**) 2-D representation of binding interaction illustrating the important amino acid residues involved in the interactions within 3Å around the ligand.

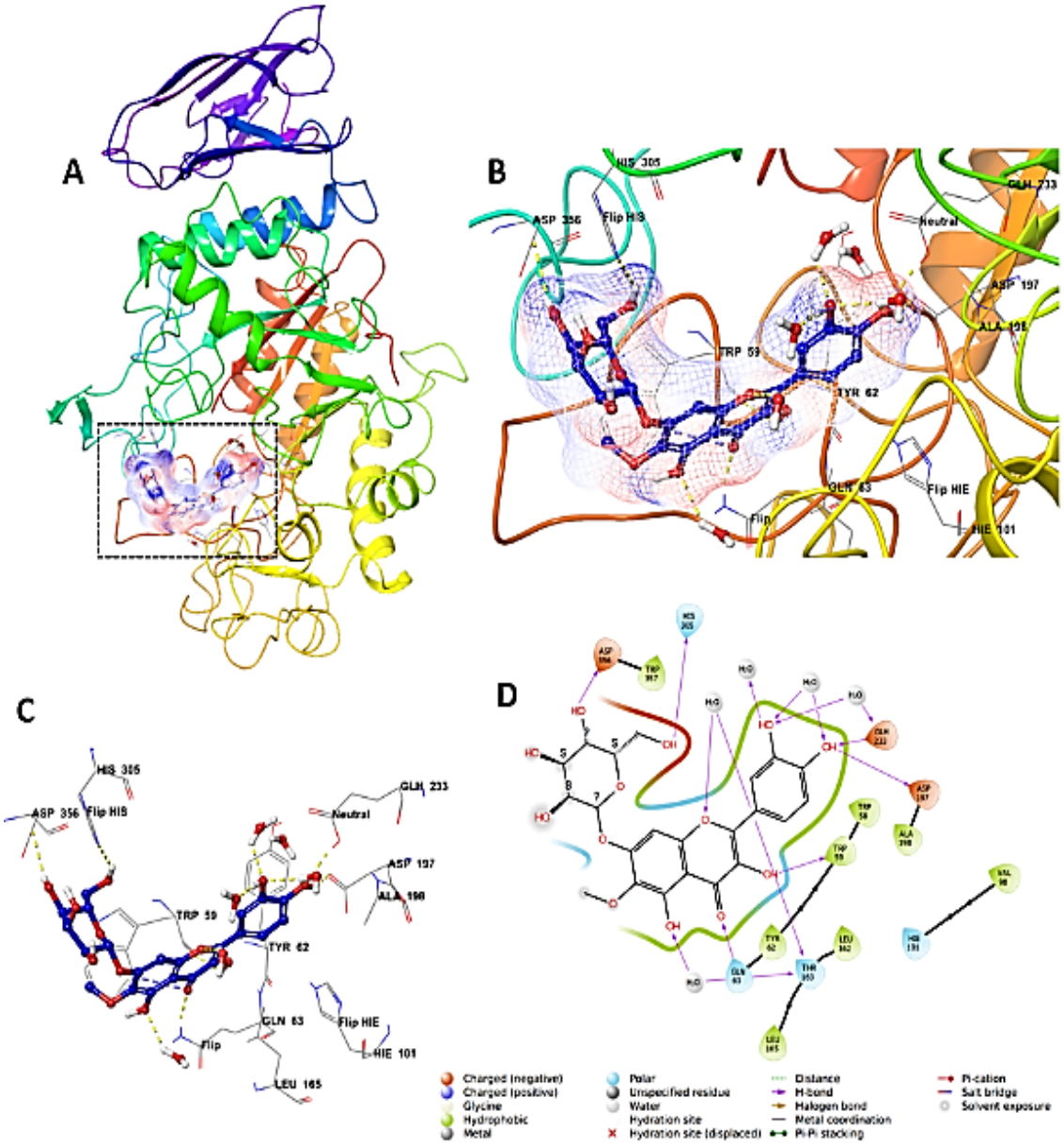

Figure 5: Patuletin-7-glucoside (**5**) bound to human AA (PDB: 4GQR). (A) Cartoon-style representation with residue position colour scheme and mesh style and electrostatic potential colour scheme for the ligand (red, white, and blue; minimum electrostatic potential: -0.3, maximum electrostatic potential: +0.3). (B) Close-up view of compound **5** bound to human AA. (C) 2-D binding interaction representation showing principal amino acid residues involved in the interaction within 3Å around the ligand. (D) 3-D profile of binding interaction showing compound **5** in green wire representation, amino acid residues in grey wire representation, aromatic hydrogen bonds in violet dots, and hydrogen bonds in yellow dots.

of AA. It also had hydrophobic interactions with Trp 58, Trp 59, and Try 62, as well as polar interactions with Gln 63 and His 305. On the other hand, compounds **1-3** showed very weak docking scores, indicating a poor binding affinity for the active site of AA.

Based on the results of docking analysis and examination of the poses reported in Figure 4, Figure 5, and Figure 6, it was found that the hydrogen bonds formed between the polar groups in the ligands and the amino acid residues in the active site were very crucial in the binding process. Moreover, the size and functional groups of each of the ligands determined how it fitted conformationally in the active site of the protein.

CONCLUSION

Compounds **1**–**5** have been isolated from the aerial parts of *T. minuta*, and their structures determined and verified using various tools.

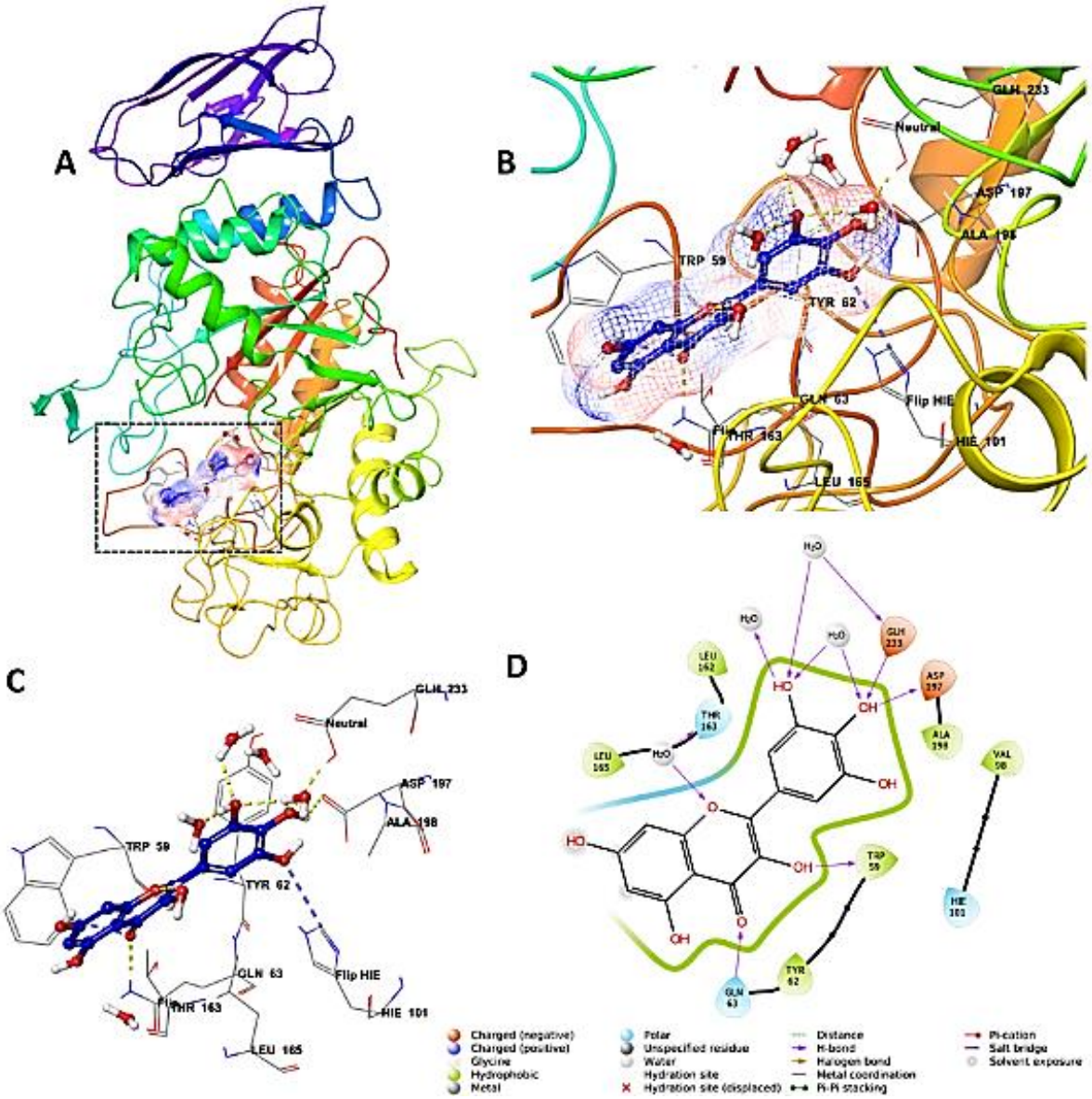

Figure 6: Myricetin in complex formation with human AA (PDB: 4GQR). (**A**) The figure shows a cartoon-style representation with a colour scheme indicating the positions of the amino acid residues. The ligand is represented as a mesh style with an electrostatic potential colour scheme (white, red, and blue), where minimum and maximum electrostatic potential values were -0.3 and +0.3, respectively. (**B**) A close-up view of the human AA binding site with myricetin is shown. (**C**) A 3-dimensional representation of the binding interaction is displayed, where myricetin is represented in green, and amino acid residues are represented using a wireframe model. Hydrogen bonds are depicted as yellow dots, and aromatic hydrogen bonds are shown as violet dots. (**D**) A 2-dimensional representation of the binding interaction showing the important amino acid residues involved in interactions within 3 Å around the ligand

Compound **1** exhibits significant cytotoxic potential against the cell lines HCT-116, MCF-7, and HepG2. Moreover, compounds **4** and **5** demonstrate potent AAI capacities. Furthermore, docking studies confirm the *in vitro* AA-inhibitory effect of these metabolites. Thus, it may be deduced that these metabolites are potential AA inhibitors. However, this assertion needs to be validated through additional *in vivo* and *in vitro* investigations.

DECLARATIONS

Acknowledgements

The Deanship of Scientific Research (DSR) at King Abdulaziz University (KAU), Jeddah, Saudi Arabia has funded this project, under Grant no. (KEP-MSc: 27-166-1443). The authors acknowledge with thanks to DSR for technical and financial support

Ethical approval

None provided.

Availability of data and materials

The datasets used and/or analyzed during the current study are available from the corresponding author on reasonable request.

Conflict of Interest

No conflict of interest associated with this work.

Contribution of Authors

This work was done by the authors named in this article, and all liabilities pertaining to claims relating to the content of this article will be borne by the authors. Gamal A Mohamed, Ali A Alqarni, Hossam M Abdallah, and Sabrin RM Ibrahim carried out the phytochemical and biological investigations. Abdelsattar M Omar performed the docking studies. All the authors contributed to the writing of the manuscript. All authors read and approved the publication of the manuscript.

Open Access

REFERENCES

1. *Shahid RK, Ahmed S, Le D, Yadav, S. Diabetes and cancer: Risk, challenges, management, and outcomes. Cancers 2021; 13: 5735.*
2. *Khan RMM, Chua ZJY, Tan JC, Yang Y, Liao Z, Zhao Y. From pre-diabetes to diabetes: Diagnosis, treatments and translational research. Medicina 2019; 55: 546.*
3. *Ling S, Brown K, Miksza JK, Howells L, Morrison A, Issa E, Yates T, Khunti K, Davies MJ, Zaccardi F. Association of type 2 diabetes with cancer: A Meta-analysis with Bias analysis for unmeasured confounding in 151 Cohorts comprising 32 million people. Diabetes Care 2020; 43: 2313-2322.*
4. *Dias DA, Urban S, Roessner U. A Historical overview of natural products in drug discovery. Metabolites 2012; 2: 303-336.*
5. *Dhalaria R, Verma R, Kumar D, Puri S, Tapwal A, Kumar V, Nepovimova E, Kuca K. Bioactive Compounds of edible fruits with their anti-aging properties: A Comprehensive review to prolong human life. Antioxidants 2020; 9: 1123.*
6. *Walia S, Kumar R. Wild marigold (Tagetes Minuta L.) an important industrial aromatic crop: Liquid gold from the Himalaya. J Essent Oil Res 2020; 32: 373-393.*
7. *Walia S, Kumar R. Wild marigold (Tagetes minuta L.) biomass and essential oil composition modulated by weed management techniques. Indust Crops Prod 2021; 161: 113183.*
8. *Ibrahim SRM, Abdallah HM, El-Halawany AM, Esmat A, Mohamed GA. Thiotagetin B and Tagetannins A and B, new acetylenic thiophene and digalloyl glucose derivatives from Tagetes minuta and evaluation of their in vitro antioxidative and anti-inflammatory activity. Fitoterapia 2018; 125: 78-88.*
9. *Ibrahim SRM, Mohamed GA, Abdel-Latif MMM, El-Messery SM, Al Musayeib NM, Shehata IA. Minutaside A, new α-amylase inhibitor flavonol glucoside from Tagetes minuta: Antidiabetic, antioxidant, and molecular modeling studies. Starch/Stärke 2015; 67: 976-984.*
10. *Al-Musayeib NM, Mohamed GA, Ibrahim SRM, Ross SA. New thiophene and flavonoid from Tagetes minuta leave growing in Saudi Arabia. Molecules 2014; 19: 2819-2828.*
11. *Ibrahim SRM, Mohamed, G.A.A. Tagetones A and B, New Cytotoxic Monocyclic Diterpenoids from Flowers of Tagetes Minuta. Chinese J Nat Med 2017; 15: 546-549.*
12. *Schrödinger, L.L.C. Schrödinger Release 2021-4: LigPrep; Schrödinger, LLC: New York, NY, USA, 2021.*
13. *Mohamed GA, Ibrahim SRM. Garcixanthone E and garcimangophenone C: New metabolites from Garcinia mangostana and their cytotoxic and alpha amylase inhibitory potential. Life (Basel). 2022; 12(11): 1875.*
14. *Dhakal RC, Rajbhandari M, Kalauni SK, Awale S, Gewali MB. Phytochemical constituents of the bark of Vitex negundo L. J Nepal Chem Soc 2009; 23: 89-92.*
15. *Abdel-Wahhab MA, Said A, Huefner A. NMR and radical scavenging activities of patuletin from Urtica urens against aflatoxin B1. Pharm Biol 2005; 43: 515-525.*
16. *Ibrahim SRM, Omar AM, Bagalagel AA, Diri RM, Noor AO, Almasri DM, Mohamed SGA, Mohamed, GA. Thiophenes-naturally occurring plant metabolites: Biological activities and in silico evaluation of their potential as cathepsin D inhibitors. Plants (Basel) 2022; 11: 539.*
17. *Sung H, Ferlay J, Siegel RL, Laversanne M, Soerjomataram I, Jemal A, Bray F. Global cancer statistics 2020: Globocan estimates of incidence and mortality worldwide for 36 cancers in 185 countries. CA: Cancer J Clin 2021;7 1: 209-249.*
18. *Alhakamy NA, Mohamed GA, Fahmy UA, Eid BG, Ahmed OAA, Al-Rabia MW, Khedr AIM, Nasrullah MZ, Ibrahim, SRM. New alpha-amylase inhibitory metabolites from pericarps of Garcinia mangostana. Life 2022; 12: 384.*

19. Ibrahim SRM Abdallah HM, El-Halawany AM, Nafady AM, Mohamed GA. Mangostanaxanthone VIII, a new Xanthone from Garcinia mangostana and its cytotoxic activity. Nat Prod Res 2019; 33: 258-265.
20. Ibrahim SRM, Mohamed GA, Khayat MT, Ahmed S, Abo-Haded H, Alshali KZ. Mangostanaxanthone VIIII, a new xanthone from Garcinia mangostana pericarps, α-amylase inhibitory activity, and molecular docking studies. Rev bras farmacogn 2019; 29: 206-212.
21. Baig MH, Ahmad K, Rabbani G, Danishuddin M, Choi I. Computer aided drug design and its application to the development of potential drugs for neurodegenerative disorders. Curr Neuropharmacol 2018; 16: 740-748.
22. Williams LK, Li C, Withers SG, Brayer GD. Order and disorder: differential structural impacts of myricetin and ethyl caffeate on human Amylase, an antidiabetic target. J Med Chem 2012; 55: 10177-10186.
23. Cavalluzzi MM, Mangiatordi GF, Nicolotti O, Lentini G. Ligand Efficiency Metrics in drug discovery: The Pros and Cons from a practical perspective. Expert Opin Drug Discov 2017; 12: 1087-1104.